JACS
JOURNAL OF THE AMERICAN CHEMICAL SOCIETY
Article
pubs.acs.org/JACS

Utilizing Redox-Mediated Bergman Cyclization toward the Development of Dual-Action Metalloenediyne Therapeutics

Sarah E. Lindahl,[†] Hyunsoo Park,[‡] Maren Pink,[‡] and Jeffrey M. Zaleski*[,†]

[†]Department of Chemistry and [‡]Molecular Structure Center, Indiana University, Bloomington, Indiana 47405, United States

Supporting Information

ABSTRACT: Reaction of 2 equiv of 1,2-bis((diphenylphosphino)ethynyl)benzene (dppeb, **1**) with $Pt(cod)Cl_2$ followed by treatment with N_2H_4 yields the reduced Pt(0) metalloenediyne, $Pt(dppeb)_2$, **2**. This complex is stable to both air oxidation and metal-mediated Bergman cyclization under ambient conditions due to the nearly idealized tetrahedral geometry. Reaction of **2** with 1 equiv of I_2 in the presence of excess 1,4-cyclohexadiene (1,4-CHD) radical trap rapidly and near-quantitatively generates the *cis*-Bergman-cyclized, diiodo product **3** (^{31}P: δ = 41 ppm, J_{Pt-P} = 3346 Hz) with concomitant loss of 1 equiv of uncyclized phosphine chelate (^{31}P: δ = −33 ppm). In contrast, addition of 2 equiv of I_2 in the absence of additional radical trap instantaneously forms a metastable $Pt(dppeb)_2^{2+}$ intermediate species, **4**, that is characterized by δ = 51 ppm in the ^{31}P NMR (J_{Pt-P} = 3171 Hz) and $\nu_{C\equiv C}$ = 2169 cm^{-1} in the Raman profile, indicating that it is an uncyclized, bis-ligated complex. Over 24 h, **4** undergoes ligand exchange to form a neutral, square planar complex that spontaneously Bergman cyclizes at ambient temperature to give the crystalline product $Pt(dppnap\text{-}I_2)I_2$ (dppnap-I_2 = (1,4-diiodonaphthalene-2,3-diyl)bis(diphenylphosphine)), **5**, in 52% isolated yield. Computational analysis of the oxidation reaction proposes two plausible flattened tetrahedral structures for intermediate **4**: one where the phosphine core has migrated to a *trans*-spanning chelate geometry, and a second, higher energy structure (3.3 kcal/mol) with two *cis*-chelating phosphine ligands (41° dihedral angle) via a restricted alkyne-terminal starting point. While the energies are disparate, the common theme in both structures is the elongated Pt−P bond lengths (>2.4 Å), indicating that nucleophilic ligand substitution by I^- is on the reaction trajectory to the cyclized product **5**. The efficiency of the redox-mediated Bergman cyclization reaction of this stable Pt(0) metalloenediyne prodrug and resulting cisplatin-like byproduct represents an intriguing new strategy for potential dual-threat metalloenediyne therapeutics.

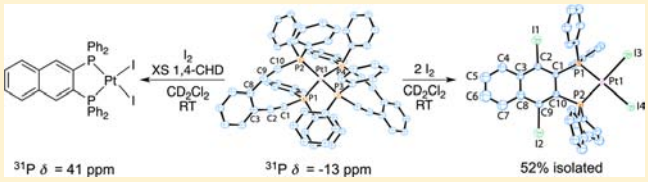

INTRODUCTION

In 1965, Rosenberg's interest in the effects of alternating current electric fields on *Escherichia coli* proliferation using Pt-mesh electrodes led to the curious observation of filamentous cell growth due to the arrest of cell division. Rosenberg traced the phenomenon to Pt(IV) and Pt(II) species generated *in situ* by oxidation of the metallic Pt electrodes within the ammonium chloride-containing growth medium. This fundamental inquiry ultimately led to the serendipitous discovery of cisplatin, (*cis*-$Pt(NH_3)_2Cl_2$), the most celebrated inorganic medicinal agent since its FDA approval in 1978.[1,2] The mechanism of action of cisplatin derives from aquation of the Pt(II) center to form a cationic complex that binds DNA predominately through 1,2-intrastrand guanine N7 (GG) cross-links that kink the DNA backbone at ∼40°, leading to disruption of DNA synthesis and ultimately cell death.[2−8]

The impact of Rosenberg's fundamental discovery has fueled development of second-generation compounds such as carboplatin and oxaliplatin.[2,7,9] Simultaneously, considerable effort has gone into probing *trans*-Pt(II) constructs,[10−12] despite the fact that transplatin itself has no therapeutic activity. Indeed, *trans*-Pt(II) structures supporting sterically hindered amines and iminoethers restore antitumor activities mirroring the action of cisplatin and, more remarkably, are active in cisplatin- and oxaliplatin-resistant cell lines.[10−12] Although considerable evidence exists for DNA platination by these complexes, their activities in cisplatin-resistant cells, combined with the lack of cell cycle interference, suggests that targets other than DNA and alternate mechanisms leading to cell death may be operative.[12]

Ligand structural compositions beyond am(m)ines, specifically Pt-phosphine or mixed phosphine/am(m)ine complexes, also show considerable antitumor activity.[13−30] Complexes with open or exchangeable coordination positions appear to operate in the more classic cisplain-like manner via DNA adduct formation,[13,18,19,21,23,26−30] while coordinatively saturated structures, especially those with chelating lipophilic phosphines, are proposed to function by a unique anti-mitochondrial mechanism.[18,19,21] This functional divergence may be the reason that these cationic complexes are active against cisplatin-resistant cells.

Rosenberg also recognized that Pt(IV) compounds may be viable as anti-proliferation agents, though many have been shown to be reduced to active Pt(II) species within the cell.[9,31,32] Nevertheless, recent chemical strategies have taken

Received: August 17, 2012
Published: February 22, 2013

   dx.doi.org/10.1021/ja308190q | J. Am. Chem. Soc. 2013, 135, 3826−3833

advantage of the solubility enhancement and favorable pharmacokinetics of redox-active Pt(IV) complexes as potential cisplatin prodrugs.[9,31−34] In addition, Pt(IV) complexes have been recognized as a viable photochemically active route to two-electron-reduced cisplatin-like structures. Here, UV photolysis of all *trans*-Pt$(N_3)_2(OH)_2$ am(m)ine/imine derivatives leads to azide-to-Pt(IV) ligand-to-metal charge transfer (LMCT), resulting in Pt(II) formation with concomitant azide radical dissociation.[35−40] While the Pt(II) product is capable of forming DNA adducts analogous to those of traditional cisplatin derivatives, the release of reactive nitrogen species is also proposed to account for cytotoxicity by an alternative autophagy mechanism.[40]

Our interest in metal-enediyne complexes bearing reactive radical-generating ligands[41−51] capable of H-atom abstraction like their parent enediyne natural products[52,53] has led to an ongoing investigation of the reactive 1,2-bis((diphenylphosphino)ethynyl)benzene (dppeb, **1**) ligand with platinum originally reported by Buchwald.[54] We have demonstrated that geometric modulation controls metal-enediyne conformations and, consequently, reactivities/stabilities toward Bergman cyclization. For comparable structure types, tetrahedral geometries are markedly more stable to Bergman cyclization than their planar metalloenediyne counterparts, to upward of 100 °C.[43,55,56] The question we propose is, can a metal-based redox process be used to rapidly and efficiently switch these stable constructs to reactive molecules capable of Bergman cyclization, similar to the way Pt(IV) LMCT photolysis leads to formation of reduced cisplatin derivatives? While redox-controlled Bergman cycloaromatization has been examined within an organic hydroquinone/quinone couple,[57] metal oxidation/reduction-triggered cyclization has not been demonstrated.

Within this theme, we report a chemical rendering of Rosenberg's original Pt-electrode oxidation to form cisplatin *in situ*. Here, oxidation of a tetrahedral Pt(0) phosphino-metalloenediyne complex generates a square planar *cis*-Pt(II) phosphine dihalide product via a reactive diradical intermediate capable of H-atom abstraction. The base Pt-phosphine structural motif parallels established Pt-phosphines with antitumor activity. More importantly, both the diradical intermediate and the final square planar product have the potential to attack biological substrates by different mechanisms and thus represent a conceptual design for the development of metal-mediated dual-threat therapies.

RESULTS AND DISCUSSION

The air-stable Pt(0) metalloenediyne, **2**, was prepared by reacting 2 equiv of **1**[54] with Pt(cod)Cl_2 followed by addition of N_2H_4 (Scheme 1). Purification and recrystallization from cold EtOH affords **2** as an orange solid that has been fully characterized in both solution and the solid state. X-ray crystallographic analysis reveals that **2** has a tetrahedral geometry about the metal center, with nearly idealized P−Pt−P angles of 109°. The interalkynyl distance, 3.46 Å, which is similar to other d^{10} homologues,[41,42] is found to be reduced relative to free ligand **1**, but increased with respect to the proposed square planar, Pt(II) analogue.[54] As a consequence, the Bergman cyclization temperature of **2** is high (231 °C) in the solid state as evaluated from the maximum of the differential scanning calorimetry trace, consistent with other tetrahedral metalloenediynes.[41−43,58]

In an effort to explore whether *in situ* oxidation can be used to promote Bergman cyclization of thermally robust d^{10} metalloenediynes, 1 equiv of I_2 was added to a solution of **2** in the presence of excess 1,4-CHD in deoxygenated CD_2Cl_2 at room temperature (Scheme 2). Immediately upon addition, an orange-to-yellow color change is observed and ^{31}P NMR reveals near quantitative conversion of the starting material (δ = −13 ppm, J_{Pt-P} = 3923 Hz) to a single platinated species, **3** (δ = 41 ppm, J_{Pt-P}: 3346 Hz) and free ligand, **1** (δ = −33 ppm, Figure 1).[59] The only other ^{31}P NMR signal observed is at δ = 6.86 ppm (∼ 7%) and can be attributed to trace formation of phosphine-iodine adducts.[60−65] The reaction is complete within 5 min and complex **3** is stable in solution as no further changes are observed in the ^{31}P NMR spectrum over a matter of 3 d.

The Pt satellites, ^{31}P chemical shift, and J_{Pt-P}: 3346 Hz indicate that **3** is a Pt(II) structure with one chelating

Scheme 1. Synthesis of Bis(1,2-bis((diphenylphosphino)ethynyl)benzene)platinum(0), 2

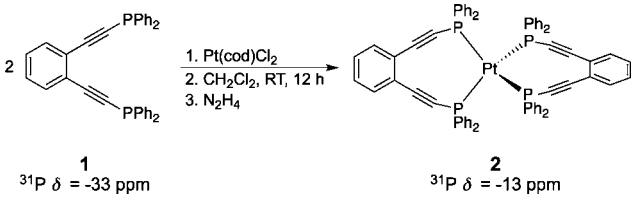

Scheme 2. Redox-Mediated Bergman Cyclization of 2 in the Presence of Excess 1,4-CHD To Yield the Benzannulated Product 3[a]

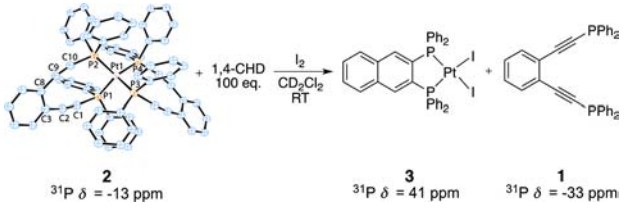

[a]Thermal ellipsoids are illustrated at 50% probability and H-atoms have been omitted for clarity.

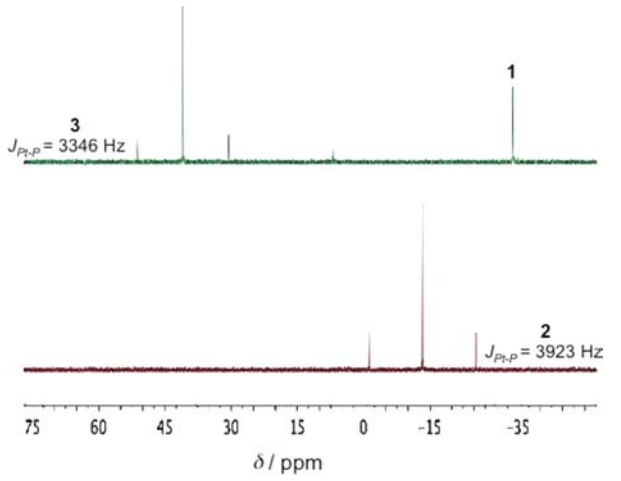

Figure 1. ^{31}P NMR spectra showing the oxidation of **2** in the presence of I_2 and excess 1,4-CHD leading to the instantaneous generation of **3** in near quantitative yield.

dx.doi.org/10.1021/ja308190q | J. Am. Chem. Soc. 2013, 135, 3826−3833

phosphine ligand.[66] To verify the ^{31}P chemical shift of the Pt(II) complex and determine the cyclization state of the ligand upon oxidation, **3** was independently synthesized by reaction of $Pt(cod)I_2$ and **1** in a 1:1 molar ratio in the presence of excess 1,4-CHD and toluene at 80 °C for 3 h (Scheme 3).[67] The

Scheme 3. Independent Synthesis of Diiodo-(2,3-bis(diphenylphosphino)naphthalene)platinum(II), 3

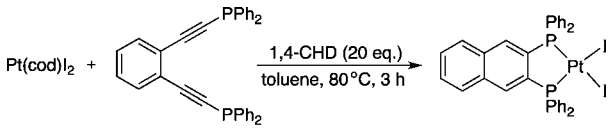

1 $^{31}P\ \delta$ = -33 ppm **3** $^{31}P\ \delta$ = 41 ppm

reaction affords the Bergman cyclized diiodo product, **3** in 82% yield, as confirmed by the loss of the alkyne carbons in the ^{13}C NMR spectrum and high-resolution mass analysis (see Experimental Section for full characterization).

Interestingly, the addition of 2 equiv of I_2 to a deoxygenated solution of **2** in CD_2Cl_2 devoid of 1,4-CHD at room temperature does not accelerate the oxidation reaction. Rather, immediately upon addition an orange-to-yellow color change is observed and ^{31}P NMR reveals quantitative conversion of the starting material (δ = −13 ppm, J_{Pt-P} = 3923 Hz) to a single phosphorus-containing species, **4** (δ = 51 ppm, J_{Pt-P} = 3171 Hz) of different chemical shift than **3** (Figure 2). After

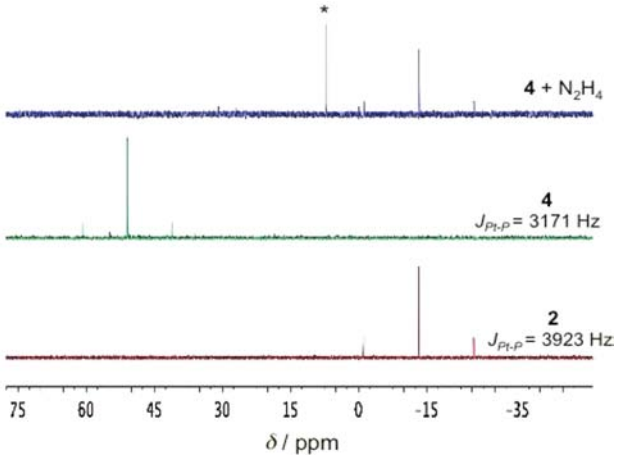

Figure 2. ^{31}P NMR spectra showing the oxidation of **2** to **4** and subsequent reduction of **4** to regenerate starting material. The designated (*) signal corresponds to the phosphine-oxide analogue of the free ligand, **6**, which is generated during the reduction reaction and has been confirmed and characterized by independent synthesis.

approximately 24 h, the ^{31}P signal corresponding to **4** decreases in intesity concomitant with the formation of a yellow crystalline precipitate, **5** (Scheme 4). Complex **5** was isolated in 52% yield and found to be insoluble in both polar and nonpolar solvents. During the precipitation of **5**, multiple weak ^{31}P signals (10−50 ppm) are observed that are attributed to phosphine-iodine adducts of the liberated phosphine ligand.[60−65]

The X-ray crystal structure of **5** reveals that this Bergman-cyclized product results from the two-electron oxidation of the platinum center by 1 equiv of iodine with loss of one phosphine-enediyne ligand to generate the diiodo cisplatin-like product. The second equivalent of I_2 serves as a stoichiometric radical trap, quenching the 1,4-diradical intermediate generated upon cyclization. From the X-ray structure of **5** it is clear that the reduced quencher concentration fortuitously reveals the presence of intermediate **4**, which is not detected during the formation of **3** with excess 1,4-CHD. Finally, the divalent metal center of **5** exhibits a nearly idealized square planar coordination environment with the naphthalene ring lying approximately 5° below the plane of the metal center.

Though **5** is confirmed as the oxidized, cyclized product, the structure and geometry of intermediate **4** with ^{31}P NMR signal at δ = 51 ppm are ambiguous. The transformation from **2** to **5** requires both oxidation and cyclization of the starting material; however, it is unclear whether those are concerted or stepwise events.

To fully understand this oxidation-induced transformation via intermediate **4**, a solution of **2** in deoxygenated CD_2Cl_2 was subject to sequential *in situ* oxidation and reduction. Upon the addition of 2 equiv of iodine, quantitative oxidation of **2** is confirmed by the presence of the ^{31}P signal at δ = 51 ppm. Immediately following oxidation, excess reducing equivalents in the form of hydrazine were added to the reaction mixture and the ^{31}P NMR spectrum acquired. The addition of N_2H_4 regenerates the starting material **2** (Figure 2), as well as the phosphine-oxide analogue of the free ligand **6**, which has been confirmed and characterized by independent synthesis.[68] The reduction of **4** back to uncyclized starting material suggests that **4** must possess uncyclized alkynes, as a long-lived diradical species is not plausible and conversion from a benzannulated product back through a diradical intermediate is an energetically uphill process.[69] Moreover, this oxidation has been found to be electrochemically reversible as shown by the single anodic, quasi-reversible wave at E_p^a = −361 mV (vs Fc/Fc^+) in the cyclic voltammogram of **2** (Figure 3), further demonstrating that **4** must be a soluble, uncyclized Pt(II) complex containing both phosphine ligands.

Off-resonance (λ = 785 nm, 2 mW) Raman spectroscopy was also used to probe the ligand functional group composition of **4** and determine whether the alkynes remain unactivated in solution (Figure 4). The Raman spectrum of **2** shows an intense alkyne stretching vibration at 2150 cm^{-1} as well as phenyl ring and 1,2-disubstituted benzene stretching and bending vibrations between 1600 and 600 cm^{-1}. The Raman spectrum of **5** is devoid of an alkyne vibration as expected due to the cyclized nature of the complex. Intense $\nu_{C=C}$ stretching modes and δ_{C-H} in-plane and out-of-plane aromatic deformations are still observed throughout the spectrum; however, the appearance of new signals at 1357 and 1319 cm^{-1}, characteristic of mono- or disubstituted naphthalenes,[70] provides an additional spectroscopic handle for the identification of cyclized enediyne moieties. The Raman spectrum of **4** is quite similar to that of **2**, with a strong, broad alkyne vibration at 2169 cm^{-1}. The presence of this feature, coupled with the lack of substituted naphthalene signals between 1400 and 1300 cm^{-1}, indicates that the *in situ* species **4** possesses uncyclized alkyne functionalities.

Though **4** could not be isolated and analyzed crystallographically, speculations regarding the geometry of this species can be made from the available experimental data. The ^{31}P NMR spectrum of **4** shows conversion to a single phosphorus-containing species implying that **4** is a four-coordinate structure, with a chemical shift indicative of a Pt(II) complex. The highly comparable Raman spectra of **2** and **4** also mandate

dx.doi.org/10.1021/ja308190q | J. Am. Chem. Soc. 2013, 135, 3826−3833

Scheme 4. Oxidation and Subsequent *in Situ* Bergman Cyclization of 2 To Generate the Benzannulated Complex 5[a]

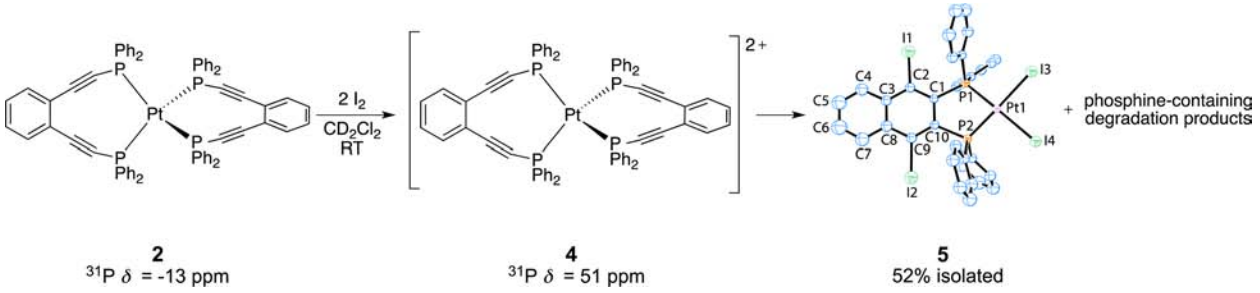

2 $^{31}P\ \delta$ = -13 ppm **4** $^{31}P\ \delta$ = 51 ppm **5** 52% isolated

[a]Thermal ellipsoids are illustrated at 50% probability and H-atoms have been omitted for clarity.

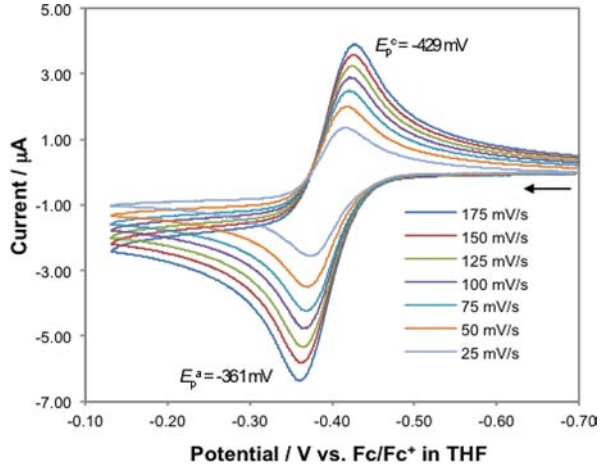

Figure 3. Cyclic voltammogram showing the quasi-reversible oxidation of **2**.

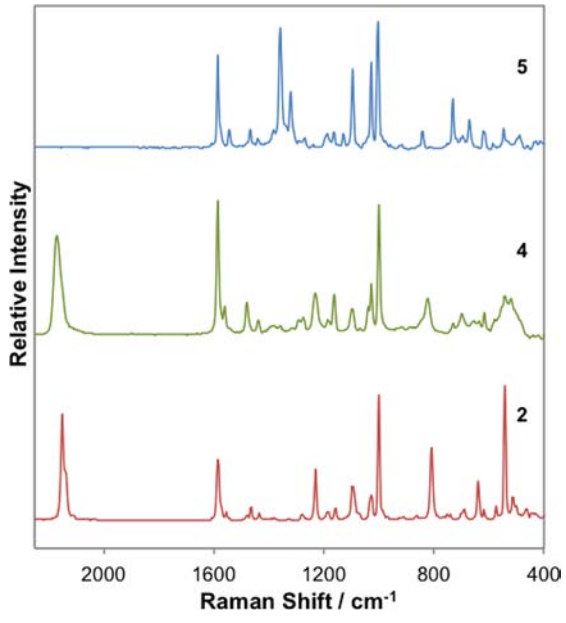

Figure 4. Off-resonance Raman spectra of complexes **2**, **4**, and **5**, obtained at 2 mW and λ = 785 nm.

similar functional group composition for these two complexes. The change in platinum oxidation state from 0 to +2 suggests an accompanying change in geometry from tetrahedral to square planar. Though crystal field theory encourages **4** to be a square planar complex, a previous study has shown square planar, d^8 metalloenediynes of **1** to be highly reactive toward Bergman cyclization at or below ambient temperatures in solution.[54] Given the reversibility of the oxidation reaction and the observation that **4** persists in solution for several days, it is unreasonable to predict that **4** adopts a perfectly square planar geometry in solution; rather, **4** must have a flattened tetrahedral ($\sim D_{2d}$) structure forming a metastable species that persists in solution. Over 24 h, intermediate **4** exchanges one phosphine chelate for two iodide ligands neutralizing the charge of the complex and relieving the strain about the metal center. This allows a reactive *cis*-square planar geometry to trigger facile Bergman cyclization *in situ* at ambient temperature. The neutral analogue then crystallizes out of deuterated dichloromethane to afford **5**.

To better envision the structural rearrangement that converts the Pt(0), tetrahedral bis-chelate complex **2**, to the Pt(II) cisplatin-like products **3** and **5** upon two-electron oxidation, as well as further probe the structure of proposed intermediate **4**, density functional theory (DFT) calculations were employed. Geometry optimizations and vibrational analyses were performed with Gaussian 09[71] using the B3LYP[72−74] density functional and an ultrafine grid. The 6-31G** basis set was used to model C, H, and P while the LANL2 pseudopotential with the LANL2DZ[75−77] basis set was applied to all metal atoms. This was followed by single point energy calculations in dichloromethane (dielectric constant ε = 8.93) using the PCM model[78−82] at the same level of theory.

The computed structure of **2** was obtained by minimization of the X-ray crystal structure of the starting material. The optimized structure of **2** contains no imaginary frequencies and the primary metal−ligand structural parameters are in good agreement with the crystallographic data. The geometry of **2** in the Pt(II) oxidation state was then used as the starting point for the optimization of intermediate **4**. To adapt to the Pt(II) oxidation state and approach a square planar geometry, the optimized structure of **4** maintains a bis-chelate with uncyclized enediyne ligands that adopt an expanded P−Pt−P angle of ∼138° toward a pseudo-*trans*-spanning configuration, which is consistent with ^{31}P NMR and Raman spectroscopic analyses (Figure 5). This distorted or flattened tetrahedron consequently increases the interalkynyl distance from 3.51 Å in **2** to 3.76 Å in **4**. Moreover, relative to **2** (∼168°) one C≡C−P angle decreases to ∼164° while the other increases to ∼171°, with the more bent C≡C−P angle corresponding to the chelate arm with the shorter Pt−P bond. An increase in the linearity of the C≡C−P angle shifts the $\nu_{C\equiv C}$ stretching vibration to higher energy, which is consistent with both the calculated and experimental Raman spectra of **4**. Vibrational analysis of **4** shows two alkyne stretching frequencies at 2158

dx.doi.org/10.1021/ja308190q | J. Am. Chem. Soc. 2013, 135, 3826−3833

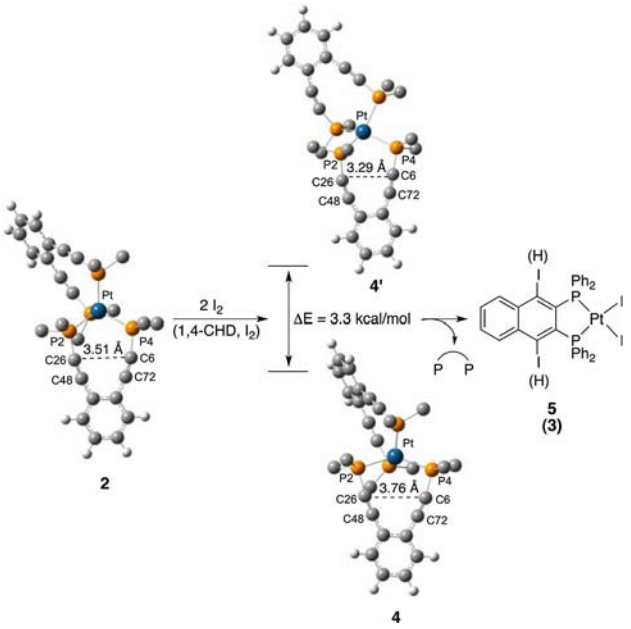

Figure 5. Reaction trajectory for generation of **5** by I_2 oxidation of **2** via computed structural intermediates **4** or **4′**. Calculated structures are viewed with the same phosphine-chelate perspective and phenyl rings at the phosphorus atoms have been reduced to only the *ipso* carbons for clarity.

and 2174 cm^{-1}, respectively, while the experimental spectrum finds a single broad $\nu_{C\equiv C}$ stretching vibration centered at 2169 cm^{-1}.

More importantly, the Pt−P bond lengths of **4** are lengthened relative to the tetrahedral starting material **2** (Pt−P ∼2.38 Å), with one Pt−P bond close to that of **2** (2.39 Å) while the other is appreciably longer at 2.45 Å. Bond elongation indicates decreased metal−ligand orbital overlap, which provides an operative pathway for ligand substitution by nucleophilic I^- to form the monochelated, cisplatin-like, cyclized diiodo product. The observation of **4** in solution by ^{31}P NMR and its 24 h metastability is consistent with a substitution-based reaction trajectory toward formation of a *cis*-planar structure and consequential Bergman cyclization.

While the structural characteristics of **4** are consistent with the reaction pathway and spectroscopically observable species, we questioned whether a planar *cis*-chelated structure for intermediate **4** is accessible via dihedral angle rotation (**4′**). To probe this structure and evaluate its energetic disposition relative to the *trans*-chelate **4**, the interalkynyl separation (C6···C26) was reduced from 3.51 Å in **2** to 3.1 Å as a geometric minimization starting point. The optimized structure of **4′** is once again a distorted tetrahedron, but with a *cis*- rather than *trans*-chelated structure like that of **4** and a dihedral angle of 41°. The P−Pt−P bond angles are accordingly reduced to ∼96°. Interestingly, all Pt−P bond lengths are markedly increased from 2.39 Å in **2** to an average of 2.47 Å for **4′** (Table 1) due to steric clashes of the phenyl rings. While the energy of this structure is 3.3 kcal/mol higher than that of **4** and the structure was realized using a constrained geometric starting point, the increase in Pt−P bond length is a reoccurring theme. This facilitates ligand substitution by I^- and formation of a transient, uncyclized Pt(II)-iodo complex that adopts a *cis*-chelate structure, which is wholly consistent with formation of *cis*-cyclized product **5** and concomitant observation of free

Table 1. Bond Angles (°) and Interatomic Distances (Å) for Complexes 2, 4, and 4′ Computed Using B3LYP/6-31G and the LANL2DZ Pseudopotential**

bond angles (deg) and lengths (Å)	2	4	4′
P4−Pt−P2	109.2	138.4	95.6
C48−C26−P2	168.6	170.9	162.5
C72−C6−P4	166.9	164.3	171.8
Pt−P4	2.38	2.39	2.49
Pt−P2	2.40	2.45	2.43
interalkynyl C6−C26	3.52	3.76	3.29

phosphine in the ^{31}P NMR. Whether the *cis*-chelated intermediate **4′** or the modestly lower energy *trans*-chelated structure **4** is the valid transient species, both routes can be expected to lead to phosphine lability and *cis*-promoted cyclization.

■ CONCLUSIONS

Analogously to Rosenberg's electrochemical generation of cisplatin, chemical oxidation of the bis-phosphinoenediyne chelated Pt(0) complex generates a transient Pt(II) species with a flattened tetrahedral geometry and elongated Pt−P bonds that is prone to phosphine ligand substitution by halide. Ligand dissociation subsequently leads to the structural freedom to adopt a *cis*-chelate conformation that spontaneously Bergman cyclizes to generate the corresponding cisplatin-like product. Redox-activated metalloenediyne prodrugs that lead to cisplatin-like species have significant potential for development into dual-mode therapeutics. While it remains to be seen what the therapeutic potential of this conceptual approach is, the diradical intermediate capable of H-atom abstraction combined with the DNA-cross-linking viability of the dihaloplatinum product suggests that coupling of these reactive elements into a triggerable, efficient molecular agent could lead to an advanced generation of cisplatin analogues, much like their redox-activated Pt(IV) counterparts.

■ EXPERIMENTAL SECTION

Materials. All reactions were carried out using standard drybox and Schlenk techniques under inert nitrogen atmosphere unless otherwise specified. All chemicals and solvents were purchased from commercial sources and used as received. Solvents were dried and distilled according to standard procedures unless otherwise noted. Deuterated solvents were dried over 4 Å molecular sieves and degassed with three cycles of freeze−pump−thaw.

Physical Measurements. NMR spectroscopy was collected on a Varian Inova 400 or 500 MHz NMR spectrometer using the residual proton resonance of the solvent as an internal reference. All ^{31}P spectra were externally referenced using an 85% H_3PO_4 standard. Mass spectrometry data were obtained on a Bruker Autoflex III MALDI-TOF mass spectrometer or an Agilent 1200 HPLC-6130 MSD mass spectrometer. Differential scanning calorimetry (DSC) measurements were made on a TGA Q10 DSC system with a TA Instruments thermal analyzer at a heating rate of 10 °C min^{-1}. Raman spectroscopic data were collected on a Renishaw 1000B micro-Raman instrument using a λ_{exc} = 785 nm excitation wavelength and analyzed using the GramsAI software package. Elemental analyses were obtained from Robertson Microlit Laboratories, Inc. X-ray crystallographic data were obtained by the Indiana University Molecular Structure Center on a Bruker APEX II Kappa Duo diffractometer using Mo Kα radiation (graphite monochromator) at 150 (**2**) and 200 K (**5**). Details of the X-ray analyses can be found in Supporting Information.

dx.doi.org/10.1021/ja308190q | J. Am. Chem. Soc. 2013, 135, 3826−3833

Electrochemical Measurements. Cyclic voltammetry (CV) experiments were carried out using a three-electrode setup with a platinum disk (2.0 mm diameter), platinum wire, and a Ag/AgCl electrode as the working (WE), auxiliary (AE), and reference electrodes (RE), respectively. Data were collected on an E2 Epsilon (BAS) Autolab potentiostat-galvanostat equipped with standard BAS software and exported to Excel for manipulation and analysis. Potentials in CV were calibrated using the Fc/Fc^+ redox couple (0.0 V). Controlled-potential (bulk) electrolyses were performed using a PARC model 173 potentiostat−galvanostat. Current−time curves were obtained with the aid of locally written Labview software and integrated with OriginPro 8.6 software to acquire coulometric n values. The potentials for coulometry experiments are quoted with respect to a reference electrode consisting of a cadmium-saturated mercury amalgam in contact with DMF saturated with both cadmium chloride and sodium chloride; this electrode has a potential of −0.76 V versus the aqueous saturated calomel electrode (SCE) at 25 °C.[83−85] The glass cell employed for potentiostatic coulometry consisted of two separate compartments. In the upper compartment, a graphite rod, which serves as the auxiliary electrode, was immersed in a 0.3 M $TBAPF_6$−THF solution, separated from the analyte by a fine-porosity sintered-glass disk and backed with a methyl-cellulose-electrolyte plug. The working electrode is attached to a metal plunger contact housed in the bottom compartment of the cell along with a stir bar to add convection. Working electrodes for controlled-potential (bulk) electrolyses were reticulated vitreous carbon discs (RVC 2X1-100S, Energy Research and Generation, Inc., Oakland, CA) approximately 17 mm in diameter and 3 mm in thickness that were cut from longer rods. Information regarding the fabrication, cleaning, and handling of these electrodes can be found elsewhere.[86] A solution of **2** (1.44 mg, 0.0012 mmol) in 10 mL of deoxygenated THF was added to the bottom compartment and the entire cell purged with argon for 15 min after which time a 1.30 V potential was applied to the cell to ensure exhaustive oxidation of **2**. The coulometric n value for the oxidation of **2** was determined to be n = 1.9 by integration of the exponential current decay vs time profile.

Computational Methods and Vibrational Analysis. Geometry optimizations and vibrational analyses were performed using DFT with the B3LYP[72−74] functional, 6-31G** basis set, and an ultrafine grid using Gaussian 09.[71] The LANL2DZ effective core potential was used to model the transition metal atoms.[75−77] Single point energy calculations in dichloromethane (dielectric constant ε = 8.93) were performed using the PCM model[78−82] at the same level of theory to account for energetic contributions from solvation. The calculated vibrational frequencies were scaled uniformly by a factor of 0.962 for comparison with the observed Raman spectra, resulting in very good overall agreement between all computational and experimental values.

Bis(1,2-bis((diphenylphosphino)ethynyl)benzene)platinum-(0) (2). To a solution of $Pt(cod)Cl_2$ (37.0 mg, 0.0989 mmol) in CH_2Cl_2 (20 mL) was added a solution of dppeb **1**[54] (96.4 mg, 0.1945 mmol) in CH_2Cl_2 (5 mL) via syringe. The solution was allowed to stir at room temperature overnight, during which time the color changed from yellow to orange. Hydrazine was added until bubbling ceased. Solvent was removed under vacuum, resulting in a crude orange solid, which was dissolved in a minimal amount of CH_2Cl_2 and precipitated using cold EtOH. Crystals suitable for characterization by X-ray crystallography were grown from vapor diffusion of diethyl ether into a saturated CH_2Cl_2 solution. Yield: 48%. NMR: δ_H (400 MHz, 298 K, CD_2Cl_2) 7.53−7.44 (m, 8H), 7.26 (d, J = 5.6 Hz, 16H), 6.99 (t, J = 7.6 Hz, 8H), 6.82 (t, J = 7.6 Hz, 16H); δ_C (500 MHz, 298 K, CD_2Cl_2) 140.2, 131.7, 131.1, 129.2, 128.1, 127.8, 125.2, 109.3, 96.4; δ_P (400 MHz, 298 K, CD_2Cl_2) −13.27 (s, J = 3923 Hz). HRMS-ESI MS: m/z 1184.2415 (M^+). DSC: 231 °C (maximum). Elemental analysis, calcd for $C_{68}H_{48}P_4Pt$: C, 68.98; H, 4.09. Found: C, 68.71; H, 3.85.

Diiodo-(2,3-bis(diphenylphosphino)naphthalene)platinum-(II) (3). The preparation of **3** was performed in a manner parallel to that of the previously synthesized dichloro analogue.[67]

Method A. To a Schlenk flask were charged **1** (94.2 mg, 0.190 mmol), $Pt(cod)I_2$ (105.9 mg, 0.190 mmol), 1,4-CHD (0.36 mL, 3.80 mmol), and 10 mL of toluene. The mixture was stirred at 80 °C for 3 h, after which time pentane (50 mL) was added. Complex **3** was isolated as a pale yellow precipitate by filtration and washed copiously with hexanes to remove residual traces of unreacted starting materials. Yield: 82%. NMR: δ_H (500 MHz, 298 K, CD_2Cl_2) 8.06 (d, J = 11.5 Hz, 2H), 7.85 (dd, J = 3 Hz, 9.5 Hz, 2H), 7.78−7.82 (m, 8H), 7.62 (dd, J = 2.5 Hz, 9.5 Hz, 2H), 7.51−7.54 (m, 4H), 7.42−7.46 (m, 8H); δ_C (500 MHz, 298 K, CD_2Cl_2) 134.7, 134.6, 132.04, 132.02, 130.2, 129.8, 129.0, 128.9, 128.8; δ_P (400 MHz, 298 K, CD_2Cl_2) 41.03 (s, J = 3346 Hz). HRMS-ESI MS: m/z 818.0236 ($M^+ - I^-$). Elemental analysis, calcd for $C_{34}H_{26}P_2I_2Pt$: C, 43.20; H, 2.77. Found: C, 43.19; H, 2.61.

Method B. A solution of **2** (2.700 mg, 0.0028 mmol) in CD_2Cl_2 (1.0 mL) was charged to an NMR tube and sealed under N_2 at room temperature. Excess 1,4-CHD (0.02 mL, 0.228 mmol) and 1 equiv of an I_2 solution (0.09 mL, 25.2 mM in CD_2Cl_2) were subsequently added, and the reaction was monitored by ^{31}P NMR spectroscopy. The addition of I_2 in the presence of **2** and 1,4-CHD led to the instantaneous and nearly quantitative generation of **3** and liberated free ligand **1**, with only ∼7% (by NMR integration) unidentified phosphorus-containing side product. No further reactions of these species were observed over several days. NMR: δ_P (400 MHz, 298 K, CD_2Cl_2) 41.03 (s, J = 3346 Hz), 6.86 (s), −33.48 (s).

Bis(1,2-bis((diphenylphosphino)ethynyl)benzene)platinum-(II) Iodide (4). A solution of $Pt(dppeb)_2$ **2** (2.500 mg, 0.00211 mmol) in dry, degassed CD_2Cl_2 (0.8 mL) was charged to an NMR tube sealed under N_2. To this was added 2 equiv of an I_2 solution (0.214 mL, 19.7 mM in CD_2Cl_2). An immediate color change was observed from orange to yellow. The reaction was monitored by ^{31}P NMR, which determined **4** to be generated in quantitative yield upon I_2 addition. NMR: δ_P (400 MHz, 298 K, CD_2Cl_2) 50.85 (s, J = 3171 Hz).

Diiodo-(1,4-diiodonaphthalene-2,3-diyl)bis(diphenylphosphine)platinum(II) (5). The oxidation of **2** with 2 equiv of I_2 was monitored over time, and after 24 h yellow crystalline material began precipitating from a solution of **4** and was isolated after 3 d. Complex **5** proved insoluble in typical polar and nonpolar solvents; however, crystals suitable for characterization by X-ray crystallography were obtained directly from the reaction mixture. Yield: 52% isolated. MALDI MS: m/z 1069.84 ($M^+ - I^-$). Elemental analysis, calcd for $C_{34}H_{24}P_2I_4Pt{\cdot}CH_2Cl_2$: C, 32.79; H, 2.04. Found: C, 32.92; H, 1.79.

(1,2-Phenylenebis(ethyne-2,1-diyl))bis(diphenylphosphine oxide) (6). To a solution of **1** (150 mg, 0.303 mmol) in degassed acetone was added excess hydrogen peroxide (30% by wt), and the mixture was allowed to stir at room temperature overnight. Solvent was removed under vacuum, resulting in a pale yellow solid. The crude product was dissolved in a minimal amount of dichloromethane, and an excess of diethyl ether was added. The mixture was allowed to stand overnight at 0 °C, resulting in a shiny, white precipitate which was washed with diethyl ether and dried *in vacuo*. Yield: 63%. NMR: δ_H (400 MHz, 298 K, CD_2Cl_2) 7.8−7.7 (m, 10H), 7.5−7.4 (m, 14H); δ_C (400 MHz, 298 K, CD_2Cl_2) 134.0, 132.8, 132.6 (d, J = 3 Hz), 131.2 (d, J = 11 Hz), 130.9, 129.2 (d, J = 14 Hz), 123.5, 102.0 (d, J = 28 Hz), 89.0, 87.4; δ_P (400 MHz, 298 K, CD_2Cl_2), 7.09 (s). HRMS-ESI MS: m/z 549.1143 ($M^+ + Na^+$). DSC: 160 °C (minimum), 293 °C (maximum).

■ ASSOCIATED CONTENT

Supporting Information

DSC traces, controlled-potential (bulk) electrolysis traces, and crystallographic data (CIF). This material is available free of charge via the Internet at http://pubs.acs.org.

■ AUTHOR INFORMATION

Corresponding Author

zaleski@indiana.edu

Notes

The authors declare no competing financial interest.

■ ACKNOWLEDGMENTS

The generous support of the National Science Foundation (CHE-0956447) is gratefully acknowledged. The authors thank members of the Mindiola (Keith Searles) and Peters (Elizabeth Wagoner) research groups for their technical assistance with the electrochemical measurements. We also thank Dr. David F. Dye as well as the Raghavachari group (Victoria Erdely) for technical assistance with the calculations and computing time.

■ REFERENCES

(1) Sherman, S. E.; Lippard, S. J. *Chem. Rev.* **1987**, *87*, 1153.
(2) Lovejoy, K. S.; Lippard, S. J. *Dalton Trans.* **2009**, 10651.
(3) Takahara, P. M.; Rosenzweig, A. C.; Frederick, C. A.; Lippard, S. J. *Nature* **1995**, *377*, 649.
(4) Takahara, P. M.; Frederick, C. A.; Lippard, S. J. *J. Am. Chem. Soc.* **1996**, *118*, 12309.
(5) Todd, R. C.; Lippard, S. J. *J. Inorg. Biochem.* **2010**, *104*, 902.
(6) Jamieson, E. R.; Lippard, S. J. *Chem. Rev.* **1999**, *99*, 2467.
(7) Wang, D.; Lippard, S. J. *Nat. Rev. Drug Discovery* **2005**, *4*, 307.
(8) Jung, Y.; Lippard, S. J. *Chem. Rev.* **2007**, *107*, 1387.
(9) Graf, N.; Lippard, S. J. *Adv. Drug Delivery Rev.* **2012**, *64*, 993.
(10) Aris, S. M.; Farrell, N. P. *Eur. J. Inorg. Chem.* **2009**, 1293.
(11) Natile, G.; Coluccia, M. *Coord. Chem. Rev.* **2001**, *216*−*217*, 383.
(12) Murphy, R. F.; Komlodi-Pasztor, E.; Robey, R.; Balis, F. M.; Farrell, N. P.; Fojo, T. *Cell Cycle* **2012**, *11*, 963.
(13) Dodoff, N.; Varbanov, S.; Borisov, G.; Spasovska, N. *J. Inorg. Biochem.* **1990**, *39*, 201.
(14) Sampedro, F.; Molins-Pujol, A. M.; Bonal, J.; Barbe, J.; Garrido, S.; Pueyo, M.; Llagostera, M.; Sanchez-Ferrando, F. *Eur. J. Med. Chem.* **1991**, *26*, 539.
(15) Apfelbaum, H. C.; Blum, J.; Mandelbaum-Shavit, F. *Inorg. Chim. Acta* **1991**, *186*, 243.
(16) Sampedro, F.; Molins-Pujol, A. M.; Ruiz, J. I.; Santalo, P.; Bonal, J.; Pueyo, M.; Llagostera, M.; Sanchez-Ferrando, F. *Eur. J. Med. Chem.* **1992**, *27*, 611.
(17) Shi, J.-C.; Yueng, C.-H.; Wu, D.-X.; Liu, Q.-T.; Kang, B.-S. *Organometallics* **1999**, *18*, 3796.
(18) Habtemariam, A.; Sadler, P. J. *Chem. Commun.* **1996**, 1785.
(19) Neplechova, K.; Kasparkova, J.; Vrana, O.; Novakova, O.; Habtemariam, A.; Watchman, B.; Sadler, P. J.; Brabec, V. *Mol. Pharmacol.* **1999**, *56*, 20.
(20) Habtemariam, A.; Parkinson, J. A.; Margiotta, N.; Hambley, T. W.; Parsons, S.; Sadler, P. J. *J. Chem. Soc., Dalton Trans.* **2001**, 362.
(21) Habtemariam, A.; Watchman, B.; Potter, B. S.; Palmer, R.; Parsons, S.; Parkin, A.; Sadler, P. J. *J. Chem. Soc., Dalton Trans.* **2001**, 1306.
(22) Henderson, W.; Alley, S. R. *Inorg. Chim. Acta* **2001**, *322*, 106.
(23) Ramos-Lima, F. J.; Quiroga, A. G.; Perez, J. M.; Font-Bardia, M.; Solans, X.; Navarro-Ranninger, C. *Eur. J. Inorg. Chem.* **2003**, 1591.
(24) Romerosa, A.; Bergamini, P.; Bertolasi, V.; Canella, A.; Cattabriga, M.; Gavioli, R.; Manas, S.; Mantovani, N.; Pellacani, L. *Inorg. Chem.* **2004**, *43*, 905.
(25) Ruiz, J.; Cutillas, N.; Vicente, C.; Villa, M. D.; Lopez, G.; Lorenzo, J.; Aviles, F. X.; Moreno, V.; Bautista, D. *Inorg. Chem.* **2005**, *44*, 7365.
(26) Messere, A.; Fabbri, E.; Borgatti, M.; Gambari, R.; Di, B. B.; Pedone, C.; Romanelli, A. *J. Inorg. Biochem.* **2007**, *101*, 254.
(27) Bergamini, P.; Bertolasi, V.; Marvelli, L.; Canella, A.; Gavioli, R.; Mantovani, N.; Manas, S.; Romerosa, A. *Inorg. Chem.* **2007**, *46*, 4267.
(28) Ramos-Lima, F. J.; Quiroga, A. G.; Garcia-Serrelde, B.; Blanco, F.; Carnero, A.; Navarro-Ranninger, C. *J. Med. Chem.* **2007**, *50*, 2194.
(29) Quiroga, A. G.; Ramos-Lima, F. J.; Alvarez-Valdes, A.; Font-Bardia, M.; Bergamo, A.; Sava, G.; Navarro-Ranninger, C. *Polyhedron* **2011**, *30*, 1646.
(30) Segapelo, T. V.; Lillywhite, S.; Nordlander, E.; Haukka, M.; Darkwa, J. *Polyhedron* **2012**, *36*, 97.
(31) Cohen, S. M.; Lippard, S. J. *Prog. Nucl. Acid Res. Mol. Biol.* **2001**, *67*, 93.
(32) Chin, C. F.; Wong, D. Y. Q.; Jothibasu, R.; Ang, W. H. *Curr. Top. Med. Chem.* **2011**, *11*, 2602.
(33) Hall, M. D.; Hambley, T. W. *Coord. Chem. Rev.* **2002**, *232*, 49.
(34) Reisner, E.; Arion, V. B.; Keppler, B. K.; Pombeiro, A. J. L. *Inorg. Chim. Acta* **2008**, *361*, 1569.
(35) Mackay, F. S.; Moggach, S. A.; Collins, A.; Parsons, S.; Sadler, P. J. *Inorg. Chim. Acta* **2009**, *362*, 811.
(36) Farrer, N. J.; Woods, J. A.; Salassa, L.; Zhao, Y.; Robinson, K. S.; Clarkson, G.; Mackay, F. S.; Sadler, P. J. *Angew. Chem., Int. Ed.* **2010**, *49*, 8905.
(37) Farrer, N. J.; Woods, J. A.; Munk, V. P.; Mackay, F. S.; Sadler, P. J. *Chem. Res. Toxicol.* **2010**, *23*, 413.
(38) Pracharova, J.; Zerzankova, L.; Stepankova, J.; Novakova, O.; Farrer, N. J.; Sadler, P. J.; Brabec, V.; Kasparkova, J. *Chem. Res. Toxicol.* **2012**, *25*, 1099.
(39) Tai, H.-C.; Brodbeck, R.; Kasparkova, J.; Farrer, N. J.; Brabec, V.; Sadler, P. J.; Deeth, R. J. *Inorg. Chem.* **2012**, *51*, 6830.
(40) Westendorf, A. F.; Woods, J. A.; Korpis, K.; Farrer, N. J.; Salassa, L.; Robinson, K.; Appleyard, V.; Murray, K.; Grünert, R.; Thompson, A. M.; Sadler, P. J.; Bednarski, P. J. *Mol. Cancer Ther.* **2012**, *11*, 1894.
(41) Coalter, N. L.; Concolino, T. E.; Streib, W. E.; Hughes, C. G.; Rheingold, A. L.; Zaleski, J. M. *J. Am. Chem. Soc.* **2000**, *122*, 3112.
(42) Schmitt, E. W.; Huffman, J. C.; Zaleski, J. M. *Chem. Commun.* **2001**, 167.
(43) Benites, P. J.; Rawat, D. S.; Zaleski, J. M. *J. Am. Chem. Soc.* **2000**, *122*, 7208.
(44) Rawat, D. S.; Zaleski, J. M. *J. Am. Chem. Soc.* **2001**, *123*, 9675.
(45) Chandra, T.; Pink, M.; Zaleski, J. M. *Inorg. Chem.* **2001**, *40*, 5878.
(46) Chandra, T.; Allred, R. A.; Kraft, B. J.; Berreau, L. M.; Zaleski, J. M. *Inorg. Chem.* **2004**, *43*, 411.
(47) Bhattacharyya, S.; Pink, M.; Baik, M.-H.; Zaleski, J. M. *Angew. Chem., Int. Ed.* **2005**, *44*, 592.
(48) Bhattacharyya, S.; Dye, D. F.; Pink, M.; Zaleski, J. M. *Chem. Commun.* **2005**, 5295.
(49) Bhattacharyya, S.; Pink, M.; Huffman, J. C.; Zaleski, J. M. *Polyhedron* **2006**, *25*, 550.
(50) Bhattacharyya, S.; Clark, A. E.; Pink, M.; Zaleski, J. M. *Inorg. Chem.* **2009**, *48*, 3916.
(51) Clark, A. E.; Bhattacharyya, S.; Zaleski, J. M. *Inorg. Chem.* **2009**, *48*, 3926.
(52) Rawat, D. S.; Zaleski, J. M. *Synlett* **2004**, *3*, 393.
(53) Bhattacharyya, S.; Zaleski, J. M. *Curr. Top. Med. Chem.* **2004**, *4*, 1637.
(54) Warner, B. P.; Millar, S. P.; Broene, R. D.; Buchwald, S. L. *Science* **1995**, *269*, 814.
(55) Rawat, D. S.; Zaleski, J. M. *Synlett* **2004**, *3*, 393.
(56) Bhattacharyya, S.; Dye, D. F.; Pink, M.; Zaleski, J. M. *Chem. Commun.* **2005**, 5295.
(57) Nicolaou, K. C.; Zeng, L. Z.; McComb, S. *J. Am. Chem. Soc.* **1992**, *114*, 9279.
(58) Rawat, D. S.; Benites, P. J.; Incarvito, C. D.; Rheingold, A. L.; Zaleski, J. M. *Inorg. Chem.* **2001**, *40*, 1846.
(59) The addition of 100 equiv of 1,4-CHD to a soluiton of **2** results in no reaction over the course of 3 h in the absence of I_2.
(60) Godfrey, S. M.; Kelly, D. G.; McAuliffe, C. A.; Mackie, A. G.; Pritchard, R. G.; Watson, S. M. *J. Chem. Soc., Chem. Commun.* **1991**, 1163.
(61) Bricklebank, N.; Godfrey, S. M.; Mackie, A. G.; McAuliffe, C. A.; Pritchard, R. G.; Kobryn, P. J. *J. Chem. Soc., Dalton Trans.* **1993**, 101.
(62) Bricklebank, N.; Godfrey, S. M.; Lane, H. P.; McAuliffe, C. A.; Pritchard, R. G.; Morenao, J.-M. *J. Chem. Soc., Dalton Trans.* **1995**, 2421.
(63) Cross, W. I.; Godfrey, S. M.; McAuliffe, C. A.; Pritchard, R. G.; Sheffield, J. M.; Thompson, G. M. *J. Chem. Soc., Dalton Trans.* **1999**, 2795.
(64) Barnes, N. A.; Godfrey, S. M.; Halton, R. T. A.; Mushtaq, I.; Pritchard, R. G. *Dalton Trans.* **2008**, 1346.

(65) In light of facts that the reaction generates **3** and **1** in a nearly 1:1 ratio and the ^{31}P NMR signal of the cyclized free ligand is ∼−14 ppm, as determined by the ACD Laboratories/PNMR prediction software, the various phosphorus-containing products observed during the precipitation of **5** can be attributed to phosphorus−iodine adducts on the basis of chemical shift.
(66) Waddell, P. G.; Slawin, A. M. Z.; Woollins, J. D. *Dalton Trans.* **2010**, *39*, 8620.
(67) Warner, B. P. Ph.D. thesis, Massachusetts Institute of Technology, 1995.
(68) The mechanism for the formation of the phosphine-oxide product has not been investigated but may logically proceed from reduction of the Pt(II) center to generate diazene products that participiate in Mitsunobu-type reactions in the presence of small amounts of water.
(69) Prall, M.; Wittkopp, A.; Fokin, A. A.; Schreiner, P. R. *J. Comput. Chem.* **2001**, *22*, 1605.
(70) Socrates, G. *Infrared and Raman Characteristic Group Frequencies*, 3rd ed.; Wiley and Sons: Chichester, 2001.
(71) Frisch, M. J.; Trucks, G. W.; Schlegel, H. B.; Scuseria, G. E.; Robb, M. A.; Cheeseman, J. R.; Scalmani, G.; Barone, V.; Mennucci, B.; Petersson, G. A.; Nakatsuji, H.; Caricato, M.; Li, X.; Hratchian, H. P.; Izmaylov, A. F.; Bloino, J.; Zheng, G.; Sonnenberg, J. L.; Hada, M.; Ehara, M.; Toyota, K.; Fukuda, R.; Hasegawa, J.; Ishida, M.; Nakajima, T.; Honda, Y.; Kitao, O.; Nakai, H.; Vreven, T.; Montgomery, J. A., Jr.; Peralta, J. E.; Ogliaro, F.; Bearpark, M.; Heyd, J. J.; Brothers, E.; Kudin, K. N.; Staroverov, V. N.; Kobayashi, R.; Normand, J.; Raghavachari, K.; Rendell, A.; Burant, J. C.; Iyengar, S. S.; Tomasi, J.; Cossi, M.; Rega, N.; Millam, J. M.; Klene, M.; Knox, J. E.; Cross, J. B.; Bakken, V.; Adamo, C.; Jaramillo, J.; Gomperts, R.; Stratmann, R. E.; Yazyev, O.; Austin, A. J.; Cammi, R.; Pomelli, C.; Ochterski, J. W.; Martin, R. L.; Morokuma, K.; Zakrzewski, V. G.; Voth, G. A.; Salvador, P.; Dannenberg, J. J.; Dapprich, S.; Daniels, A. D.; Farkas, O.; Foresman, J. B.; Ortiz, J. V.; Cioslowski, J.; Fox, D. J. *Gaussian 09*; Gaussian, Inc.: Wallingford, CT, 2009.
(72) Becke, A. D. *Phys. Rev. A* **1988**, *38*, 3098.
(73) Lee, C.; Yang, W.; Parr, R. G. *Phys. Rev. B: Condens. Matter.* **1988**, *37*, 785.
(74) Becke, A. D. *J. Chem. Phys.* **1993**, *98*, 5648.
(75) Hay, P. J.; Wadt, W. R. *J. Chem. Phys.* **1985**, *82*, 270.
(76) Wadt, W. R.; Hay, P. J. *J. Chem. Phys.* **1985**, *82*, 284.
(77) Hay, P. J.; Wadt, W. R. *J. Chem. Phys.* **1985**, *82*, 299.
(78) Miertus, S.; Scrocco, E.; Tomasi, J. *Chem. Phys.* **1981**, *55*, 117.
(79) Miertus, S.; Tomasi, J. *Chem. Phys.* **1982**, *65*, 239.
(80) Pascual-Ahuir, J. L.; Silla, E.; Tuñón, I. *J. Comput. Chem.* **1994**, *15*, 1127.
(81) Cossi, M.; Barone, V.; Cammi, R.; Tomasi, J. *Chem. Phys. Lett.* **1996**, *255*, 327.
(82) Tomasi, J.; Mennucci, B.; Cammi, R. *Chem. Rev.* **2005**, *105*, 2999.
(83) Marple, L. W. *Anal. Chem.* **1967**, *39*, 844.
(84) Manning, C. W.; Purdy, W. C. *Anal. Chim. Acta* **1970**, *51*, 124.
(85) Hall, J. L.; Jennings, P. W. *Anal. Chem.* **1976**, *48*, 2026.
(86) Vanalabhpatana, P.; Peters, D. G. *J. Electrochem. Soc.* **2005**, *152*, E222.